



Generalized spin-independent WIMP-nucleus scattering from chiral effective field theory

Philipp Klos

with M. Hoferichter, J. Menéndez and A. Schwenk

Preparing for Dark Matter Particle Discovery
Chalmers University of Technology, June 12, 2018



European Research Council
Established by the European Commission



Dark matter direct detection analyses are based on input from nuclear physics

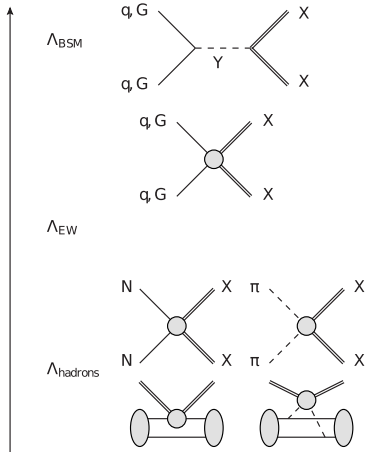
$$\frac{d\sigma}{dq^2} \propto |\langle \text{final} | H_{\chi\text{-nucleus}} | \text{initial} \rangle|^2$$

Two tasks:

Description of initial and final nuclear states

Description of WIMP-nucleus interaction

Scales of WIMP-nucleus interaction



1. BSM scale: WIMPs couple to quarks and gluons via exchange particles

2. Effective Lagrangian:

$$\mathcal{L} = \mathcal{L}_{\text{SM}} + \sum_{i,k} \frac{1}{\Lambda_{\text{BSM}}^i} \mathcal{O}_{i,k}$$

3. Integrate out EW physics

4. Chiral EFT:
WIMP couples to nucleons and pions
Embedding chiral EFT operators in nucleus

Interplay of particle, hadronic and nuclear physics scales

General WIMP-nucleus scattering cross-section:

$$\frac{d\sigma}{dq^2} \propto \left| \sum_i c_i \mathcal{F}_i \right|^2,$$

c_i embedding of WIMP couplings to quarks, gluons in hadrons

$\mathcal{F}_i^2 \propto | \langle \text{final} | H_{\chi\text{-nucleus}} | \text{initial} \rangle |^2$ structure factor

Describing nuclei

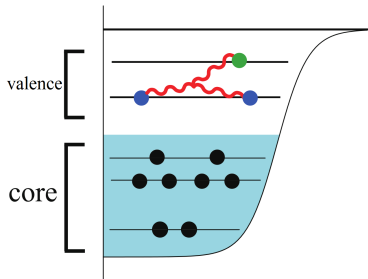
Interacting Shell Model

Separate space in

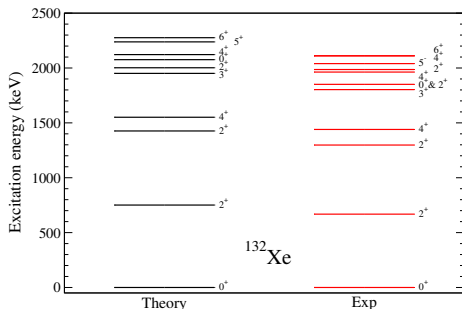
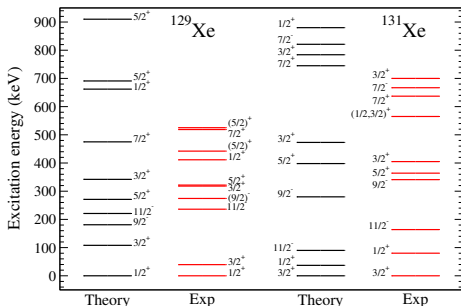
- ▶ **Outer space:** orbits that are always empty
 - ▶ **Valence space:** orbits with some nucleons but not completely filled
 - ▶ **Inner core:** orbits that are always filled
- ▶ Create effective Hamiltonian in valence space H_{eff} with effects of core and outer space perturbatively included

$$H|\Phi\rangle = E|\Phi\rangle \quad \rightarrow \quad H_{\text{eff}}|\Psi\rangle = E|\Psi\rangle$$

- ▶ \rightarrow Diagonalize H_{eff} in valence space
- ▶ \rightarrow ISM code ANTOINE [Caurier et al., RMP \(2005\)](#)



Xenon spectra



- ▶ Phenomenological interactions adjusted to nuclei in the same mass region
- ▶ Good agreement between experimental data and theory

Dark matter direct detection analyses are based on input from nuclear physics

$$\frac{d\sigma}{dq^2} \propto |\langle \text{final} | H_{\chi\text{-nucleus}} | \text{initial} \rangle|^2$$

Two tasks:

Description of initial and final nuclear states

Description of WIMP-nucleus interaction

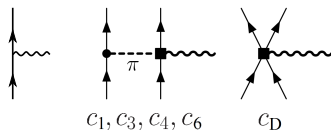
Chiral effective field theory

- ▶ Based on chiral symmetry of QCD
- ▶ Expansion in powers of Q/Λ_b (power counting)
- ▶ Chiral EFT describes consistently both nuclear forces and currents

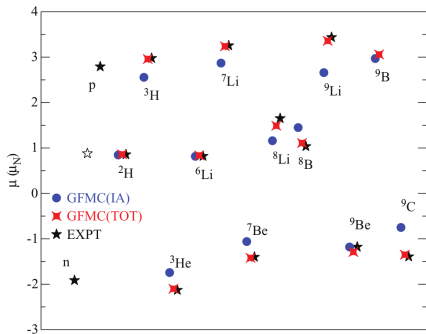
Epelbaum, Hammer, and Meißner, *RMP* **81**, 1773 (2009)

- ▶ Same low-energy constants appear in nuclear forces and currents

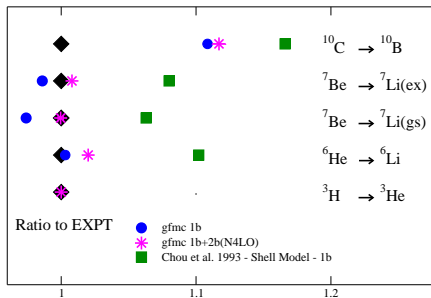
	2N force	3N force	4N force
LO		—	—
NLO		—	—
N ² LO			—
N ³ LO			



Chiral currents for magnetic moments and weak transitions



Pastore *et al.*, PRC **87**, 035503 (2013)



Pastore *et al.*, PRC **97**, 022501(R) (2018)

► Chiral two-body currents necessary to reach experimental data

Traditional WIMP responses

Spin-independent interaction: Scalar-scalar coupling: $\mathcal{L}_{\chi N} = S_\chi S_N$

WIMPs couple to nuclear density ($\mathbb{1}_\chi \mathbb{1}_N$)

$$\left| \sum^A \langle \mathcal{N} | \mathbb{1}_N | \mathcal{N} \rangle \right|^2 = A^2$$

Coherent sum over nucleons in the nucleus

Spin-dependent interaction: Axial-vector–axial-vector: $\mathcal{L}_{\chi N} = (\mathbf{A}_\chi)_\mu (\mathbf{A}_N)^\mu$

Nuclear pairing: Two spins couple to $S=0$

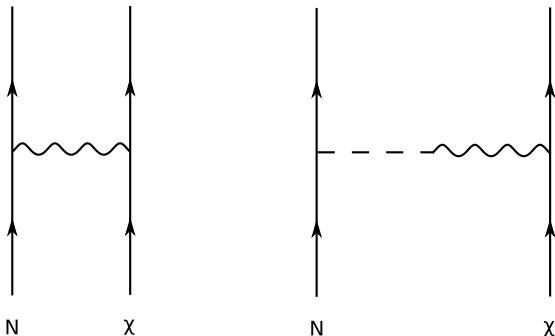
$$\left| \sum^A \langle \mathcal{N} | \mathbf{S}_N | \mathcal{N} \rangle \right|^2 = \langle \mathbf{S}_n \rangle^2, \langle \mathbf{S}_p \rangle^2$$

Cross section scale set by **spin expectation value** of odd numbered species of nucleons

Nuclear currents from chiral EFT

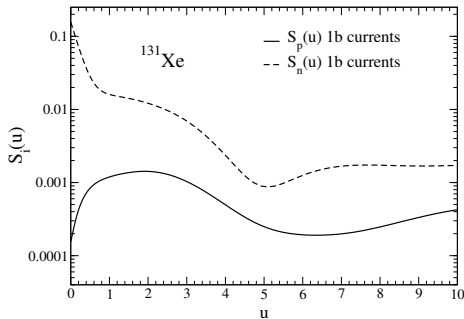
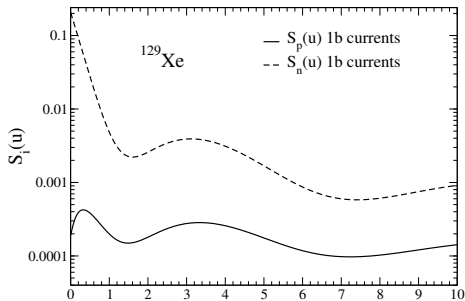
One-body current

Spin-dependent interaction: WIMP spins couple to the nuclear spin



One-body current: WIMP couples to a single nucleon.

Structure factors: Spin-dependent scattering



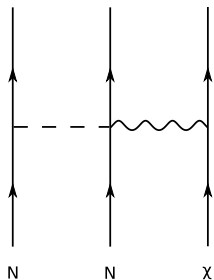
$u = q^2 b^2 / 2$ with harmonic oscillator length b

^{129}Xe		^{131}Xe	
$\langle \mathbf{S}_p \rangle$	$\langle \mathbf{S}_n \rangle$	$\langle \mathbf{S}_p \rangle$	$\langle \mathbf{S}_n \rangle$
0.010	0.329	-0.009	-0.272

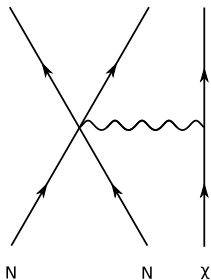
Nuclear currents from chiral EFT

Two-body currents

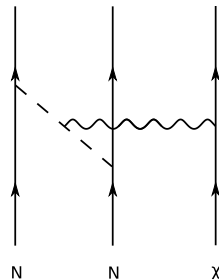
At order Q^3 , 2b currents enter:



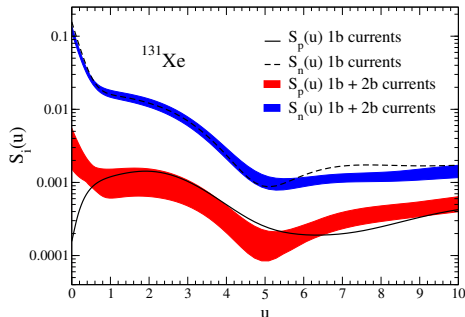
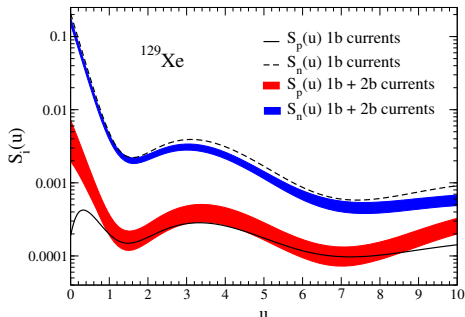
spin dependent



spin independent



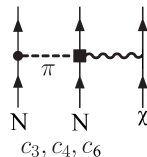
Structure factors: Spin-dependent scattering



$u = q^2 b^2 / 2$ with harmonic oscillator length b

- ▶ 2b currents \rightarrow at low momentum transfer neutrons contribute to proton structure factor $S_p(u)$
- ▶ $S_n(u)$ reduced by 20% for low momentum transfers

PK, Menéndez, Gazit, Schwenk, PRD **88**, 083516 (2013)

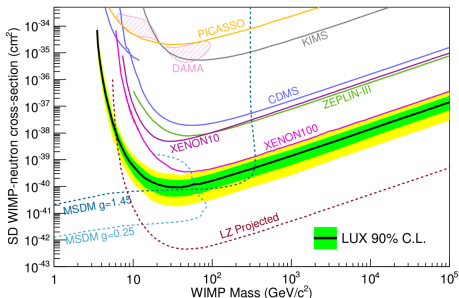


Spin-dependent limits: WIMP-neutron

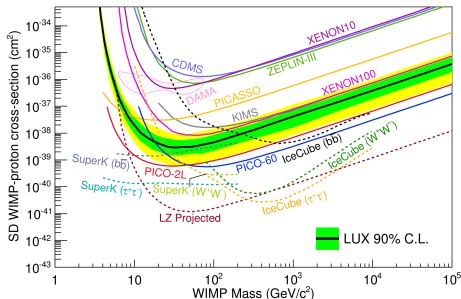
Structure factors and uncertainties in currents used in spin-dependent analysis:

LUX, PRL **116** 161302 (2016)

WIMP-neutron

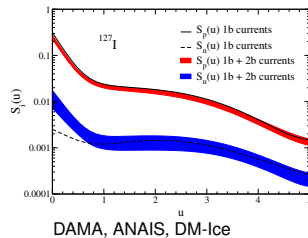
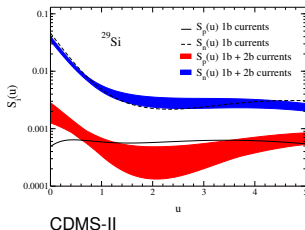
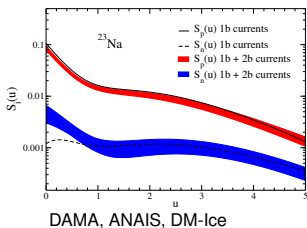
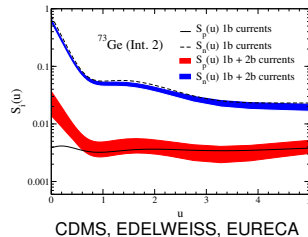
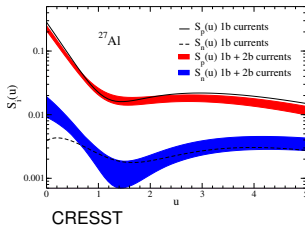
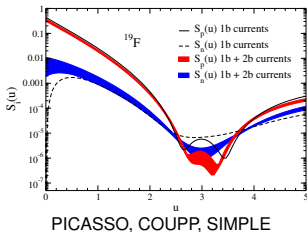


WIMP-proton

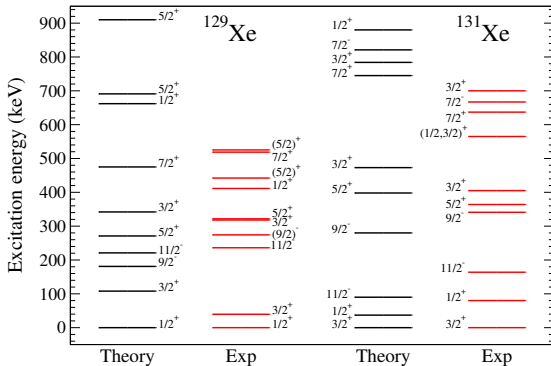


2b currents make LUX competitive for SD WIMP-proton cross-section.

SD Structure factors for different isotopes



Inelastic scattering Xenon spectra



- ▶ Excitation to low-lying first excited state (40 keV / 80 keV) possible
- ▶ Nuclear recoil + prompt deexcitation gamma can be observed

Distinguish SI and SD scattering: Inelastic scattering

Spin-independent

Elastic: $\langle \text{initial} | \sum_i^A \mathcal{L}_{\chi N}^{\text{SI}} | \text{initial} \rangle \propto A$

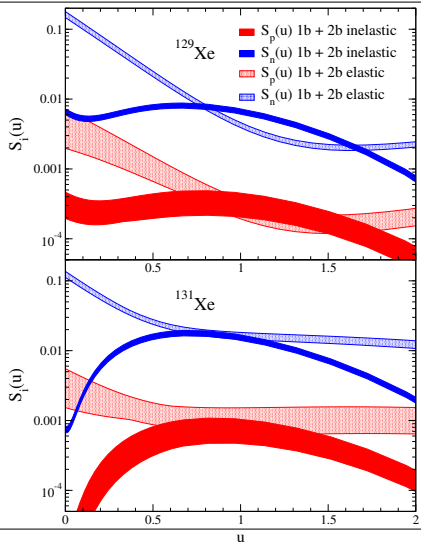
Inelastic: $\langle \text{final} | \sum_i^A \mathcal{L}_{\chi N}^{\text{SI}} | \text{initial} \rangle \propto 1$

Spin-dependent

Elastic: $\langle \text{initial} | \sum_i^A \mathcal{L}_{\chi N}^{\text{SD}} | \text{initial} \rangle \propto 1$

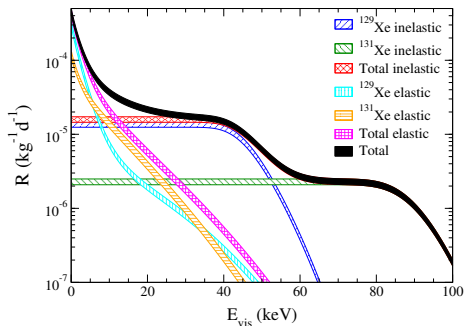
Inelastic: $\langle \text{final} | \sum_i^A \mathcal{L}_{\chi N}^{\text{SD}} | \text{initial} \rangle \propto 1$

**SD channel sensitive to both
elastic and inelastic scattering**



Inelastic scattering

Integrated recoil spectra



Mass [GeV]	^{129}Xe	^{131}Xe	Total
10	–	–	–
25	5	–	5
50	7	17	9
100	7	24	12
250	9	32	19
500	11	35	24

TABLE II. Minimum energy E_{vis} in keV above which the observed inelastic spectrum for ^{129}Xe , ^{131}Xe and for the total spectrum starts to dominate the elastic one for various WIMP masses.

- ▶ Combined information from elastic and inelastic channel will allow to **determine dominant interaction channel in one experiment**
- ▶ **Inelastic excitation sensitive to WIMP mass**

Baudis, Kessler, PK, Lang, Menéndez, Reichard, Schwenk, PRD **88**, 115014 (2013)

General WIMP responses

Spin-independent interaction:

$$\text{Scalar-scalar coupling: } \mathcal{L}_{\chi N} = S_{\chi} S_N$$

Spin-dependent interaction:

$$\text{Axial-vector-axial-vector coupling: } \mathcal{L}_{\chi N} = (A_{\chi})_{\mu} (A_N)^{\mu}$$

General WIMP-nucleon interaction Hamiltonian:

$$\mathcal{L}_{\chi N} = (V_{\chi} + A_{\chi})_{\mu} (V_N + A_N)^{\mu} + (S_{\chi} + P_{\chi})(S_N + P_N) + \dots$$

V vector

A axial-vector

S scalar

P pseudoscalar

... tensor, spin-2, ...

General WIMP responses

Chiral power counting

Combined counting of WIMP-Nucleon scattering amplitude

WIMP	Nucleon		V	A	
	t	\mathbf{x}	t	\mathbf{x}	
V	1b	0	1 + 2	2	0 + 2
	2b	4	2 + 2	2	4 + 2
	2b NLO	—	—	5	3 + 2
A	1b	0 + 2	1	2 + 2	0
	2b	4 + 2	2	2 + 2	4
	2b NLO	—	—	5 + 2	3

WIMP	Nucleon		S	P
	t	\mathbf{x}	t	\mathbf{x}
S	1b	2	2	1
	2b	4	3	5
	2b NLO	—	—	4
P	1b	2 + 2	2 + 2	1 + 2
	2b	4 + 2	3 + 2	5 + 2
	2b NLO	—	—	4 + 2

Hoferichter, PK, Schwenk, PLB **746**, 410 (2015).

- ▶ WIMP mass counted like nucleon mass
→ "+2" due to non-rel. expansion of WIMP fields
- ▶ More than only scalar-scalar and axial-vector–axial-vector up to Q^3
- ▶ **Coherence effects not included:** $\langle \text{initial} | \sum_i^A H_{\chi N}^{SI} | \text{initial} \rangle \propto A$
→ **Can easily overcome suppression in Q**



Matching to NREFT

One-body operator basis in NREFT [Fitzpatrick, et al., JCAP \(2013\)](#), [Anand et al., PRC \(2014\)](#)

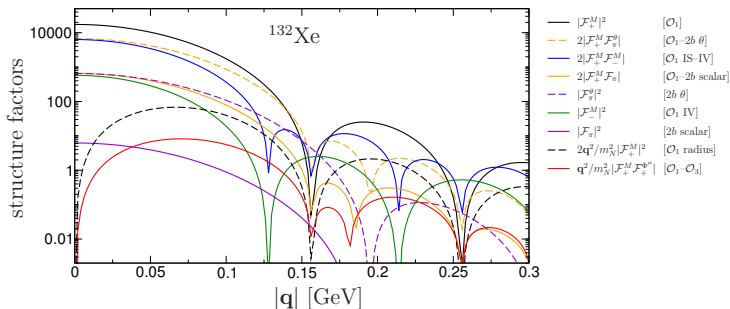
$$\begin{aligned}\mathcal{O}_1 &= \mathbb{1}, & \mathcal{O}_2 &= (\mathbf{v}^\perp)^2, & \mathcal{O}_3 &= i\mathbf{S}_N \cdot (\mathbf{q} \times \mathbf{v}^\perp), & \mathcal{O}_4 &= \mathbf{S}_\chi \cdot \mathbf{S}_N, \\ \mathcal{O}_5 &= i\mathbf{S}_\chi \cdot (\mathbf{q} \times \mathbf{v}^\perp), & \mathcal{O}_6 &= \mathbf{S}_\chi \cdot \mathbf{q} \mathbf{S}_N \cdot \mathbf{q}, & \mathcal{O}_7 &= \mathbf{S}_N \cdot \mathbf{v}^\perp, & \mathcal{O}_8 &= \mathbf{S}_\chi \cdot \mathbf{v}^\perp, \\ \mathcal{O}_9 &= i\mathbf{S}_\chi \cdot (\mathbf{S}_N \times \mathbf{q}), & \mathcal{O}_{10} &= i\mathbf{S}_N \cdot \mathbf{q} & \mathcal{O}_{11} &= i\mathbf{S}_\chi \cdot \mathbf{q}\end{aligned}$$

Matching of NREFT operators \mathcal{O}_i to chiral currents:

$$\begin{aligned}\mathcal{M}_{1,\text{NR}}^{\text{SS}} &= \mathcal{O}_1 f_N(t) \quad \text{(SI)}, & \mathcal{M}_{1,\text{NR}}^{\text{SP}} &= \mathcal{O}_{10} g_5^N(t), & \mathcal{M}_{1,\text{NR}}^{\text{PP}} &= \frac{1}{m_\chi} \mathcal{O}_6 h_5^N(t) \\ \mathcal{M}_{1,\text{NR}}^{\text{VV}} &= \mathcal{O}_1 \left(f_1^{V,N}(t) + \frac{t}{4m_N^2} f_2^{V,N}(t) \right) + \frac{1}{m_N} \mathcal{O}_3 f_2^{V,N}(t) + \frac{1}{m_N m_\chi} \left(t \mathcal{O}_4 + \mathcal{O}_6 \right) f_2^{V,N}(t) \\ \mathcal{M}_{1,\text{NR}}^{\text{AV}} &= 2\mathcal{O}_8 f_1^{V,N}(t) + \frac{2}{m_N} \mathcal{O}_9 \left(f_1^{V,N}(t) + f_2^{V,N}(t) \right) \\ \mathcal{M}_{1,\text{NR}}^{\text{AA}} &= -4\mathcal{O}_4 g_A^N(t) + \frac{1}{m_N^2} \mathcal{O}_6 g_P^N(t) \quad \text{(SD)}, & \mathcal{M}_{1,\text{NR}}^{\text{VA}} &= \left[-2\mathcal{O}_7 + \frac{2}{m_\chi} \mathcal{O}_9 \right] h_A^N(t).\end{aligned}$$

Chiral EFT: Not all \mathcal{O}_i independent & Two-body currents missing!

Extension of SI analyses

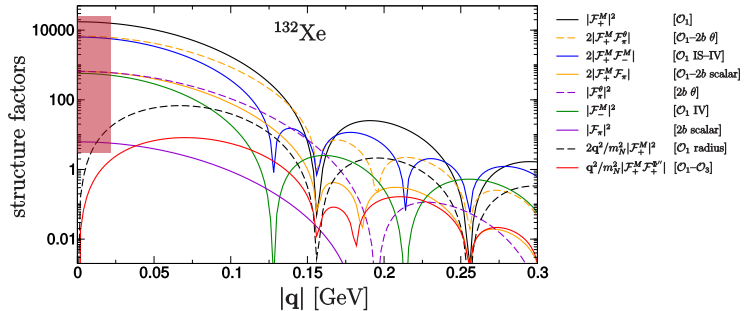


Minimal extension based QCD and **coherence** effects:

$$\frac{d\sigma_{\chi\mathcal{N}}^{\text{SI}}}{d\mathbf{q}^2} = \frac{1}{4\pi\mathbf{v}^2} \left| \left(c_+^M - \frac{\mathbf{q}^2}{m_N^2} \dot{c}_+^M \right) \mathcal{F}_+^M(\mathbf{q}^2) + c_\pi \mathcal{F}_\pi(\mathbf{q}^2) + c_\pi^\theta \mathcal{F}_\pi^\theta(\mathbf{q}^2) + \left(c_-^M - \frac{\mathbf{q}^2}{m_N^2} \dot{c}_-^M \right) \mathcal{F}_-^M(\mathbf{q}^2) \right. \\ \left. + \frac{\mathbf{q}^2}{2m_N^2} \left[c_+^{\Phi''} \mathcal{F}_+^{\Phi''}(\mathbf{q}^2) + c_-^{\Phi''} \mathcal{F}_-^{\Phi''}(\mathbf{q}^2) \right] \right|^2,$$



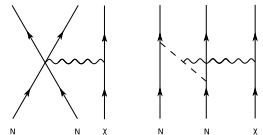
Extension of SI analyses



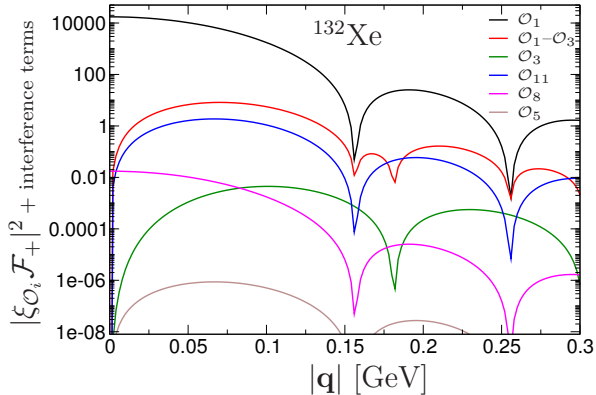
► **Dominant corrections are QCD effects:**

scalar two-body currents \mathcal{F}_π , \mathcal{F}_π^θ ,
isovector correction \mathcal{F}_-^M , radius correction

► First new operator \mathcal{O}_3 contribution is 4 orders smaller



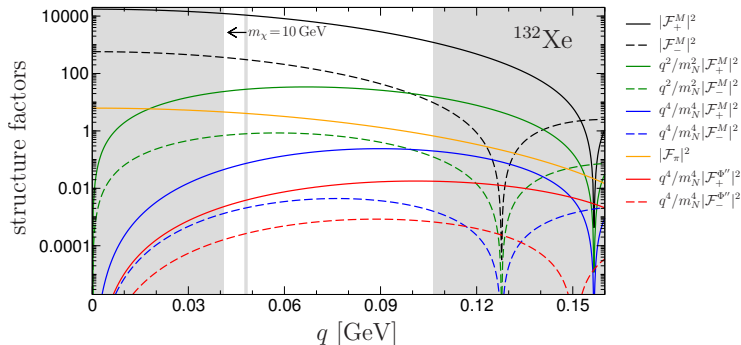
Extension of SI analyses



- ▶ Coherence effects determine hierarchy among the different operators
- ▶ Operators that vanish at $q = 0$ are less important for direct detection

Discriminating WIMP-nucleus interactions

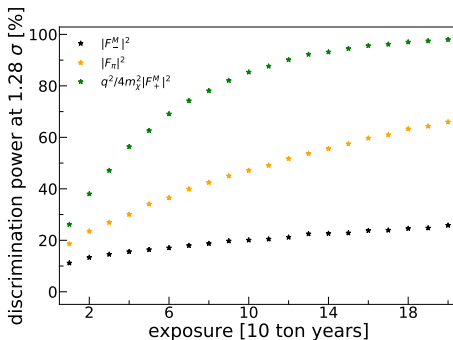
Is it possible to discriminate the different dominant response functions from the standard SI channel in XENON1T, XENONnT, or DARWIN?



Fieguth, Hoferichter, PK, Menéndez, Schwenk, Weinheimer PRD **97**, 103532 (2018)

Discriminating WIMP-nucleus interactions

q -dependence determines which responses are more easily distinguishable



Fieguth, Hoferichter, PK, Menéndez, Schwenk, Weinheimer PRD **97**, 103532 (2018)

Discriminating WIMP-nucleus interactions

TABLE III: Discrimination power (in %) of a DARWIN-like experiment after 200 ton years of exposure.

m_χ σ_0 [cm ²]	100 GeV			1 TeV		
	10 ⁻⁴⁶	10 ⁻⁴⁷	10 ⁻⁴⁸	10 ⁻⁴⁵	10 ⁻⁴⁶	10 ⁻⁴⁷
$ \mathcal{F}_-^M ^2$	94	26	12	100	35	13
$q^2/4m_\chi^2 \mathcal{F}_+^M ^2$	100	100	34	100	100	41
$q^2/4m_\chi^2 \mathcal{F}_-^M ^2$	100	98	25	100	100	32
$q^4/m_N^4 \mathcal{F}_+^M ^2$	100	100	55	100	100	63
$q^4/m_N^4 \mathcal{F}_-^M ^2$	100	100	47	100	100	53
$ \mathcal{F}_\pi ^2$	100	66	17	100	81	20
$q^4/4m_N^4 \mathcal{F}_+^{\Phi''} ^2$	100	100	58	100	100	69
$q^4/4m_N^4 \mathcal{F}_-^{\Phi''} ^2$	100	100	55	100	100	64

DARWIN could discriminate most responses unless WIMP-nucleon cross section very small

Conclusion

- ▶ State-of-the-art large-scale shell-model calculations used to predict SI / SD and extended SI WIMP responses
- ▶ Extension of standard WIMP responses beyond standard SI/SD requires QCD constraints (via chiral EFT)
- ▶ Nuclear structure predicts hierarchy amongst different responses
Hoferichter, PK, Menéndez, Schwenk, PRD **94**, 063505 (2016)
- ▶ Future detectors will be able to discriminate subleading responses from SI response
Fieguth, Hoferichter, PK, Menéndez, Schwenk, Weinheimer, PRD **97**, 103532 (2018)
- ▶ Improved limits from Higgs-portal searches
Hoferichter, PK, Menéndez, Schwenk, PRL **119**, 181803 (2017)

